Electronic Supplementary Material (ESI) for ChemComm.

Supporting Information

Pyrochlore-structural $Nd_2Ta_2O_5N_2$ Photocatalyst with Absorption Edge of over 600 nm for Z-scheme Overall Water Splitting

Hai Zou,[ab#] Yu Qi,[a#] Shiwen Du,[a] Lifang Liu,[ab] Xueshang Xin,[ab] Yunfeng Bao,[a] Shuowen Wang,[a] Zhaochi Feng[a] and Fuxiang Zhang*[a]

[a] *State Key Laboratory of Catalysis, Dalian Institute of Chemical Physics, Chinese Academy of Sciences, Dalian National Laboratory for Clean Energy, Dalian 116023, China.*

[b] *University of Chinese Academy of Sciences, Beijing 100049, China.*

[#] These authors contributed equally.

1. Experimental section

1.1 Chemical Reagents. Neodymium oxide (Nd_2O_3) was obtained from Shanghai Aladdin Biochemical Technology Co., Ltd. Tantalum oxide (Ta_2O_5) and tungsten oxide (WO_3) were purchased from High Purity Chemical. Methanol (CH_3OH) and chloroplatinic acid hexahydrate ($H_2PtCl_6.6H_2O$) were produced by Sinopharm Chemical Reagent Co., Ltd. Sodium rhodium chloride dodecahydrate ($Na_3RhCl_6.12H_2O$) and potassium iodine (KI) were obtained from Alfa Aesar. Potassium chlorine (KCl) was got from Macklin. Ruthenium trichloride ($RuCl_3$) and iridium chloride hexahydrate ($H_2IrCl_6.6H_2O$) were obtained from Tianjin Heath Biochemical Technology Co., Ltd, Dalian Kaimei Chemical Engineering Co., Ltd. and Tianjin Comiou Chemical Reagent Co., Ltd, respectively. Without special instructions, these reagents were analytically pure. The deionized (DI) water used was 18.2 MΩ.

1.2 Preparation of materials.

1.2.1 Preparation of $Nd_2Ta_2O_5N_2$. Pyrochlore-structural $Nd_2Ta_2O_5N_2$ was prepared by nitriding $NdTaO_4$ oxide precursor. Firstly, $NdTaO_4$ oxide precursor was synthesized by a flux method. Equimolar Nd_2O_3 and Ta_2O_5 were mixed with KCl of equal quality in a mortar. After grinding for 0.5 h in the presence of ethanol, grind for another 0.5 h under dry conditions to ensure uniform mixing. Then, the mixture was transformed into an alumina crucible and heated to 1150 °C for 5 h at a heating rate of 10 °C min^{-1} in a muffle furnace. After cooling down, the $NdTaO_4$ oxide precursor was obtained by washing out KCl using DI water. Dry it at 60 °C for 24 h. The $NdTaO_4$ powder was transferred into an alumina combustion boat and heated to 950 °C at a heating rate of 10 °C min^{-1} in a tube furnace, reacting for 5 h under the flow of NH_3 (50 ml min^{-1}). After cooling down, $Nd_2Ta_2O_5N_2$ powder was collected.

1.2.2 Deposition of cocatalysts. For hydrogen evolution, Pt, Ir, Rh and Ru were used as the cocatalyst. The cocatalyst was deposited on $Nd_2Ta_2O_5N_2$ by impregnation followed by hydrogen reduction method. Typically, $Nd_2Ta_2O_5N_2$ powder was ultrasonically dispersed in 2 mL H_2O including the calculated amount of metal precursor ($H_2PtCl_6.6H_2O$, $H_2IrCl_6.6H_2O$, $Na_3RhCl_6.12H_2O$ or $RuCl_3$). After drying in a water bath at 80 °C under constant stirring, it was conducted at 200 °C for 1 h under the flow of 5% H_2/95% Ar (V/V) (200 mL min^{-1}). The PtO_x was deposited on the surface of WO_3 as the cocatalyst for reduction of IO_3^- ions in the Z-scheme system.[1] WO_3 was ultrasonically dispersed in 2 mL H_2O including a calculated amount of $H_2PtCl_6.6H_2O$. After drying at 80 °C, it was calcinated at 550 °C for 0.5 h in a muffle. Then 1% CsCl in a molar ratio of WO_3 was impregnated on 0.5 *wt*% PtO_x/WO_3, following calcination at 500 °C for 10 min in a muffle. Finally, the powder was stirring in 1 M H_2SO_4 for 1 h. Wash out the residual H_2SO_4 by DI H_2O and dry the powder.[1] For water oxidation half reaction, CoO_x was deposited on $Nd_2Ta_2O_5N_2$ by two-step calcination as cocatalyst.[2] $Nd_2Ta_2O_5N_2$ powder was ultrasonically dispersed in 2 mL H_2O including a calculated amount of $Co(NO_3)_2.6H_2O$. After steaming to dry on 80 °C water bath, it was calcinated at 700 °C for 1h under the flow of NH_3 (100 mL min^{-1}). When cooling down, the powder was calcinated at 200 °C for 1 h in the air.

1.3 Characterization. Powder X-ray diffraction (XRD) was carried out on a SmartLab X-ray diffractometer (Cu Kα radiation, $\lambda = 1.5418$ Å). The diffraction date for two theta ranging from 10° to 80° were recorded at the speed of 20° per minute. High-quality data was collected with 0.01° per step to conduct the Rietveld refinement. The XRD refinement was performed on a General Structure Analysis System (GSAS) software.[3] Morphology and element distribution mapping were recorded on a JSM-7900F field emission scanning electron microscope (SEM) and a HT7700 transmission electron microscopy (TEM). X-ray photoelectron spectroscopy (XPS) was employed to acquire valence states of elements on an ESCALAB Xi + X-ray photoelectron spectrometer (Al Kα X-ray, hν = 1486.6 eV). The surface area was calculated from N_2 adsorption–desorption experiment on a Quadrasorb evo. Ultraviolet-visible (UV-vis) diffuse reflectance absorption spectroscopy (DRS) was characterized on a JASCOV-650 UV-vis diffuse reflectance spectrometer with $BaSO_4$ powder as background. And the wavelength of switching the light source from the tungsten lamp to deuterium lamp is 323 nm.

1.4 Computational details. All first-principles calculations were carried out based on the density functional theory (DFT) and the Perdew-Burke-Eznerhof generalized gradient approximation (PBE-GGA)[4, 5]. The projector augmented wave (PAW)[6, 7] scheme as incorporated in the Vienna Ab initio Simulation Package (VASP)[8, 9] was used, and a plane-wave expansion for the basis set with a cutoff energy of 500 eV was employed. The convergence criteria for the force and electronic self-consistent iteration were set to 0.02 $eV \cdot Å^{-1}$ and 1.0×10^{-5} eV, respectively. The Brillouin zone was sampled by a Monkhorst-Pack[10] of 3 × 3 × 3 K-point grid for bulk $Nd_2Ta_2O_5N_2$. The PBE + U approach was employed to accurately describe the electron states of f and d electrons, and the U values for Nd 4f and Ta 5d states were chosen as 6.0 eV and 4.5 eV according to the previous reports[11, 12], respectively.

1.5 Photocatalytic Performance. The photocatalytic reaction was carried out in a typical Pyrex top-illuminated reactor. The reactor was connected with a gas circulation system and a gas chromatography system. A certain amount of the sample was ultrasonically dispersed in the aqueous solution (20 *vol*% methanol for H_2 evolving half reaction, 10 mM $AgNO_3$ for O_2 evolving half reaction and 1 mM KI for Z-scheme overall water splitting). The air in the reactor was completely removed by pumping before photocatalytic reaction. The solution was maintained at 15 °C by circulating cold water during the reaction. A 300 W Xenon lamp was employed as the light source with a filter to cut off ultraviolet light. The amount of gas evolution was detected by a thermal conductivity detector in a gas chromatography (GC-2014, Shimadzu). The apparent quantum efficiency (AQE) at 420 nm was calculated by the equation AQE = (AR/I) ×100%, where A represents a coefficient (2 for H_2 evolution), R represents the evolution rate of H_2 in the initial one hour irradiation in a proton reduction reaction and I represents the absorption rate of incident photons. The total number of incident photons at a monochromatic wavelength of 420 nm was measured to be 1.50×10^{20} photons h^{-1}.

1.6 Electrochemical and photoelectrochemical analysis. Mott-Schottky measurements were performed on a Princeton electrochemical workstation in 0.5 M Na_2SO_4. For the preparation of the working electrode, 10 mg sample was ultrasonically dispersed in 1 mL ethanol with 10 μL 5 *wt*% nafion solution. The suspension was dropped on a 1×2 cm^2 fluorine-doped tin oxide (FTO) conductive glass. Then the as-preparaed electrode was heated at 450 °C for 1 h under N_2 atmosphere. A Pt sheet was used as the counter electrode and an Ag/AgCl electrode was used as the reference electrode. The current-potential curve was performed in 0.5 M Na_2SO_4 solution with a scan speed of 2 mV S^{-1} and switched between dark and light irradiation every 10 s.

2. Results of characterizations

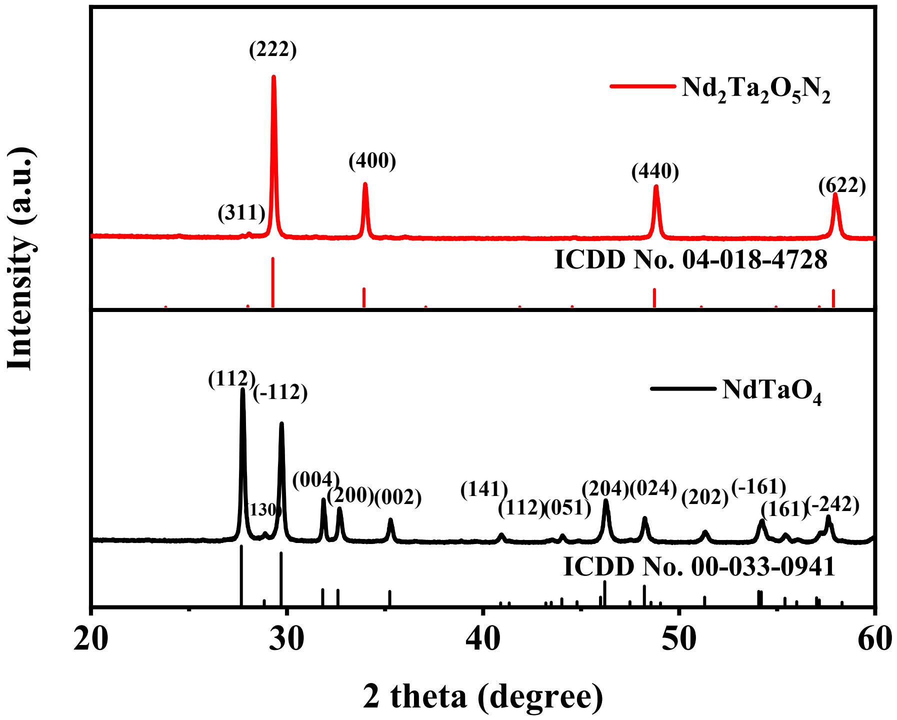

Fig. S1 XRD patterns of as-prepared $NdTaO_4$ and $Nd_2Ta_2O_5N_2$.

Table S1 Atomic coordinate information obtained from Rietveid refinement

Entry	Atom	name	x	y	z	Occ.	Wiffock	Sym.
1	Nd	Nd1	0.5	0.5	0.5	1	16d	.-3m
2	Ta	Ta2	0	0	0	1	16c	.-3m
3	O	O3	0.35627	0.125	0.125	0.714	48f	2.m m
4	N	N4	0.30141	0.125	0.125	0.286	48f	2.m m
5	O	O5	0.375	0.375	0.375	0.714	8b	-43m
6	N	N6	0.375	0.375	0.375	0.286	8b	-43m

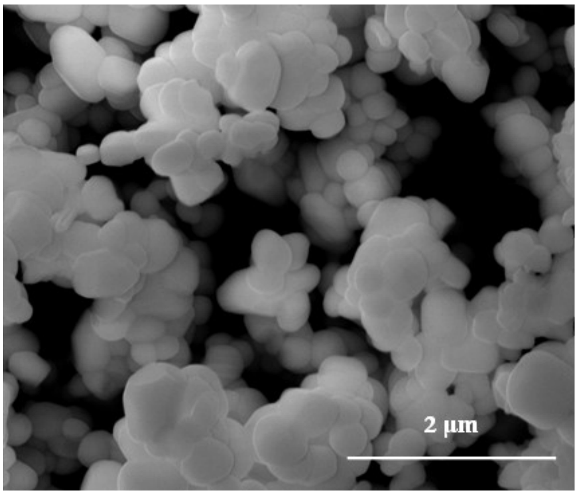

Fig. S2 SEM image of $NdTaO_4$.

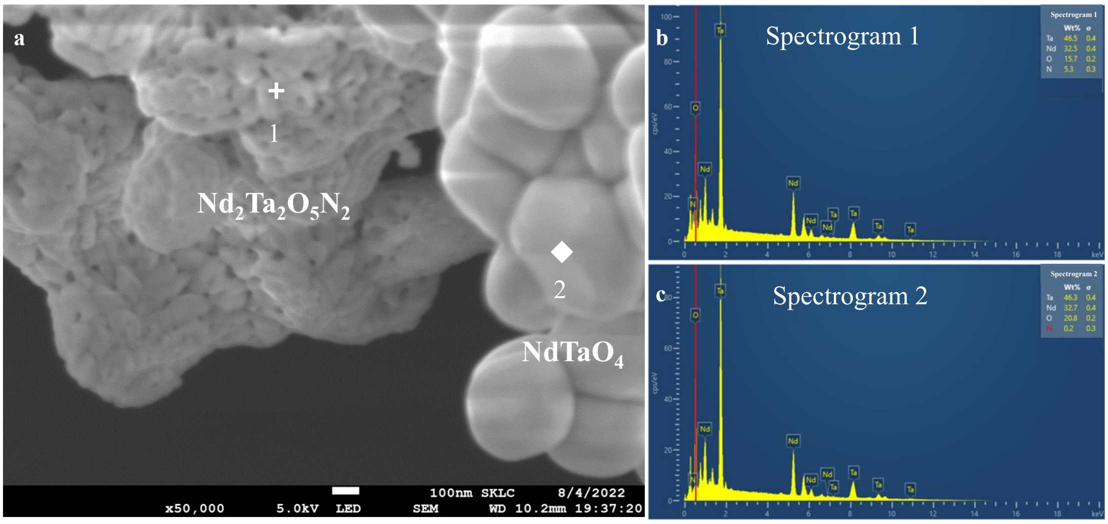

Fig. S3 (a) SEM image of mixture $Nd_2Ta_2O_5N_2$ and $NdTaO_4$. The energy dispersive X-ray spectrum (EDS) of position 1 (b) and position 2 (c) (inset: mass percentage of Nd, Ta, O and N).

To rule out the possibility that the N signal is from the background, the mechanical mixture of $Nd_2Ta_2O_5N_2$ and $NdTaO_4$ was prepared for the comparison. As shown in Fig. 1c and Fig. S2, the morphologies of $Nd_2Ta_2O_5N_2$ and $NdTaO_4$ are different. So it is easy to distinguish between $Nd_2Ta_2O_5N_2$ and $NdTaO_4$ in the mixture. The energy dispersive X-ray spectrums (EDS) of the positions from different morphologies were analyzed. As shown in Fig. S3b and c, the N element content is

5.3 *wt*% in position 1 ($Nd_2Ta_2O_5N_2$), while in position 2 ($NaTaO_4$) is only 0.2 *wt*%, which indicates the N signal from $Nd_2Ta_2O_5N_2$ is not from the background.

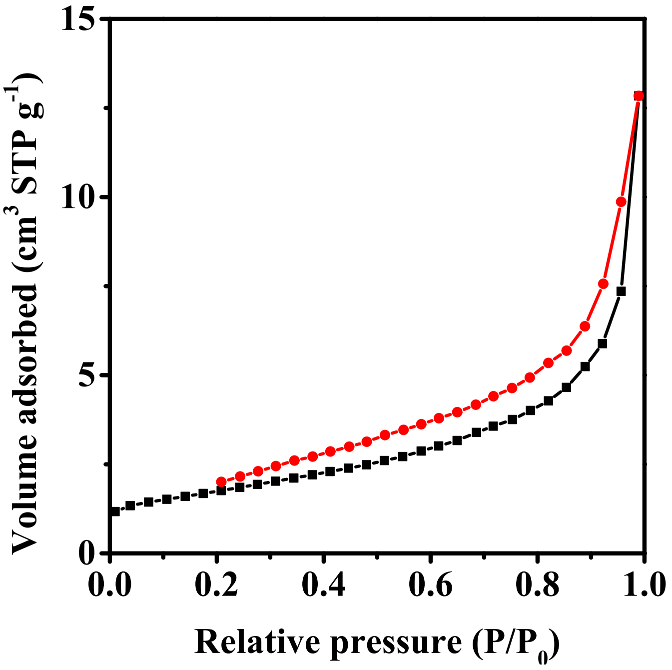

Fig. S4 N_2 adsorption–desorption isotherms of $Nd_2Ta_2O_5N_2$.

There was no obvious capillary coagulation effect from the N_2 adsorption and desorption result shown in Fig. S4. So it is considered that those pores in $Nd_2Ta_2O_5N_2$ (Fig. 1c) are macroporous architectures.

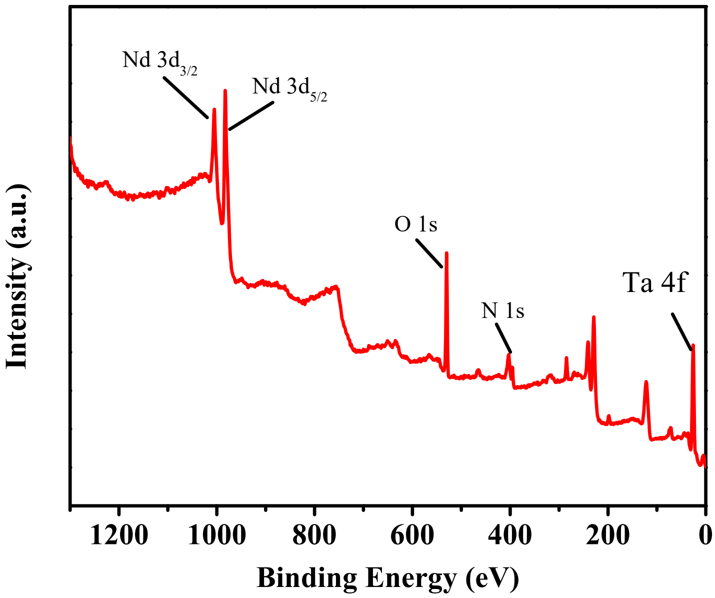

Fig. S5 XPS survey spectrum of $Nd_2Ta_2O_5N_2$.

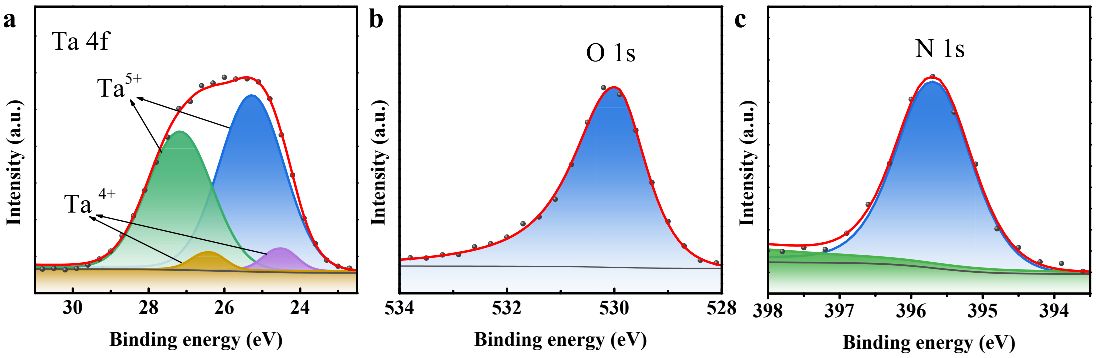

Fig. S6 High-resolution XPS spectra of Ta 4f (a), O 1s (b) and N 1s (c) of $Nd_2Ta_2O_5N_2$.

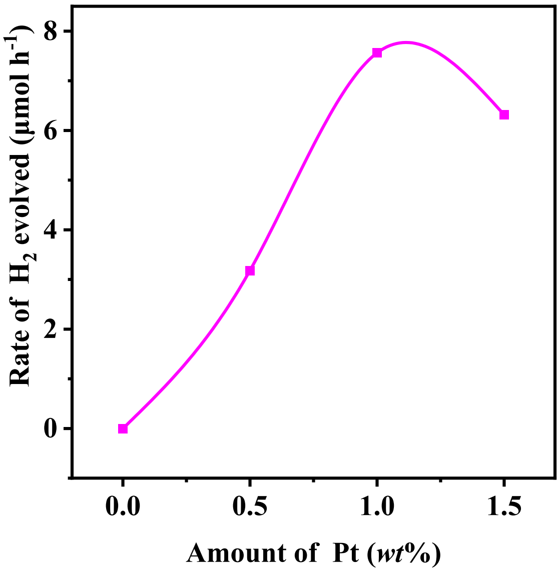

Fig. S7 Rate of H_2 evolution on $Pt/Nd_2Ta_2O_5N_2$ as a function of Pt loading amount (calculated with metal amount).

Conditions: 150 mg photocatalyst, 120 mL H_2O, 30 mL CH_3OH, 300 W Xe lamp with a cutoff filter ($\lambda \geq 420$ nm).

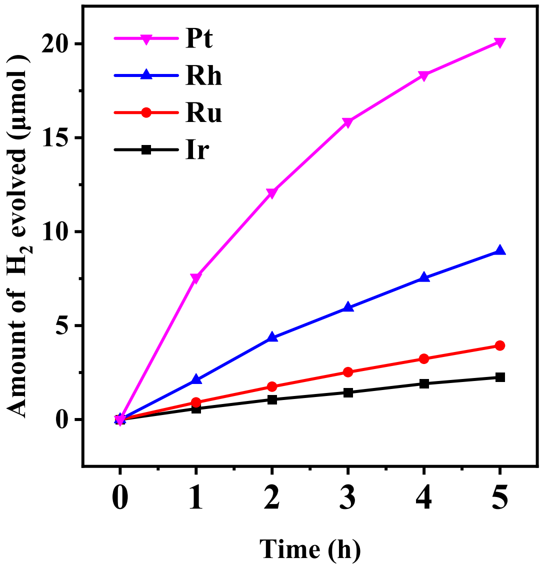

Fig. S8 Time course of H_2 evolved on $Nd_2Ta_2O_5N_2$ with different kinds of cocatalyst loaded. The loading amount is 1 *wt*%.

Conditions: 150 mg photocatalyst, 120 mL H_2O, 30 mL CH_3OH, 300 W Xe lamp with a cutoff filter ($\lambda \geq 420$ nm).

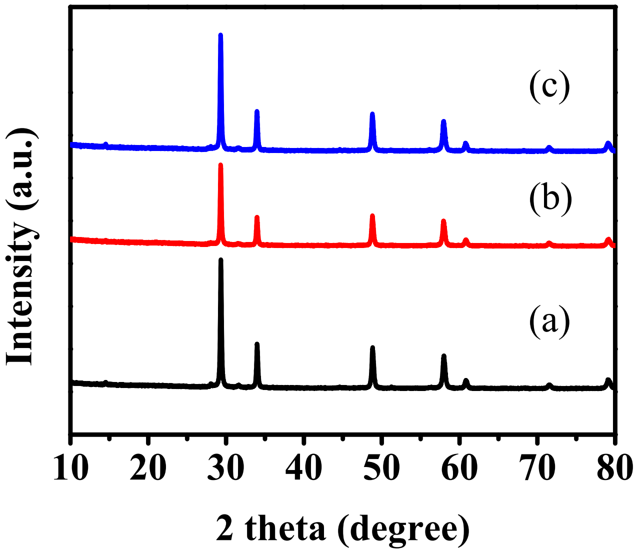

Fig. S9 XRD patterns of (a) $Nd_2Ta_2O_5N_2$, (b) 1 *wt*% $Pt/Nd_2Ta_2O_5N_2$ and (c) 1 *wt*% $Pt/Nd_2Ta_2O_5N_2$ after photocatalytic proton reduction reaction for 5 h.

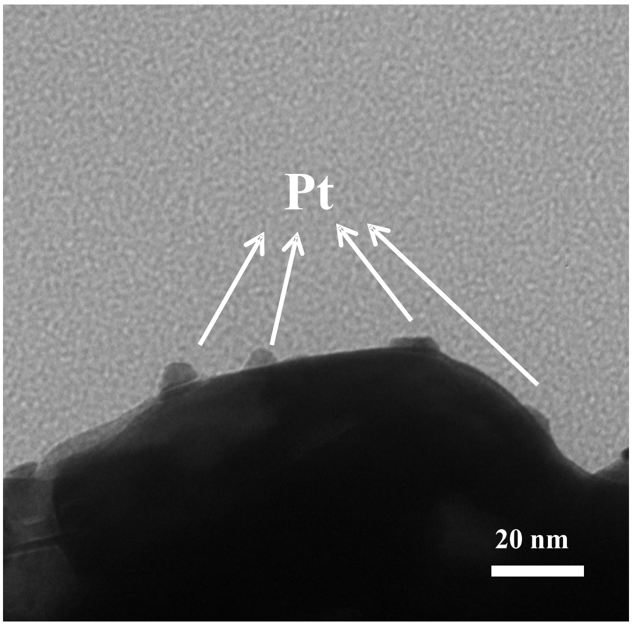

Fig. S10 TEM image of 1 *wt*% Pt/$Nd_2Ta_2O_5N_2$.

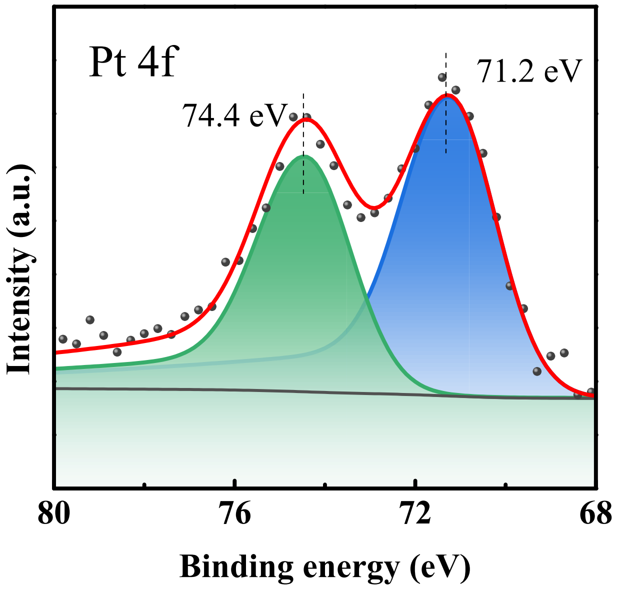

Fig. S11 High-resolution XPS spectra of Pt 4f of 1 *wt*% Pt/$Nd_2Ta_2O_5N_2$.

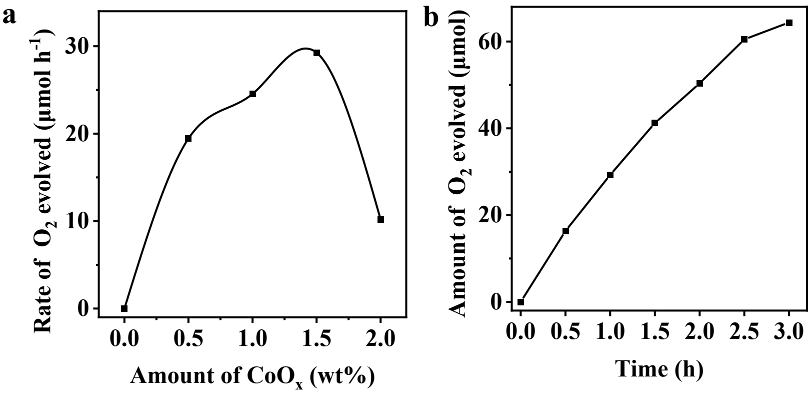

Fig. S12 Photocatalytic performance of O_2 evolution. (a) Rate of O_2 evolution on $CoO_x/Nd_2Ta_2O_5N_2$ as a function of CoO_x loading amount (calculated with metal amount); (b) Time course of O_2 evolved with 1.5 *wt*% CoO_x loading on $Nd_2Ta_2O_5N_2$. Reaction condiction: 150 mg photocatalyst; 150 mL H_2O; 1.5 mmol $AgNO_3$; 0.15 g La_2O_3; 300 W Xe lamp with a cutoff filter (λ ≥ 420 nm).

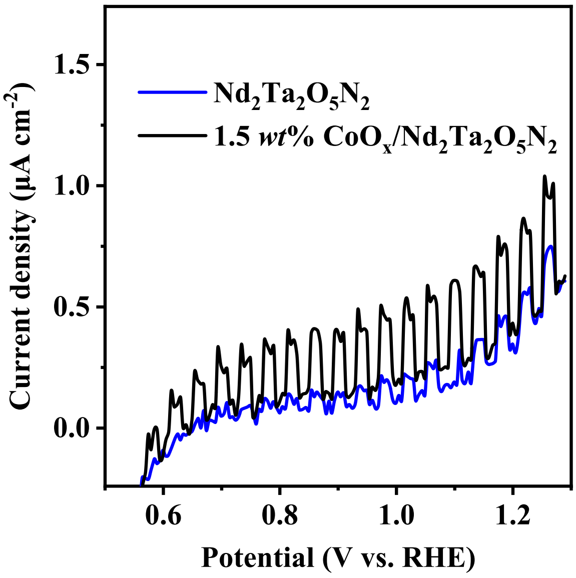

Fig. S13 Current-potential curve of $Nd_2Ta_2O_5N_2$ and 1.5 *wt*% CoO_x/ $Nd_2Ta_2O_5N_2$ Condition: 0.5 M Na_2SO_4 aqueous solution, chopped irradiation under visible light (λ ≥ 420 nm).

Notes and References

1. Y. Miseki, S. Fujiyoshi, T. Gunji and K. Sayama, *Catal. Sci. Technol.*, 2013, **3**, 1750.
2. F. Zhang, A. Yamakata, K. Maeda, Y. Moriya, T. Takata, J. Kubota, K. Teshima, S. Oishi and K. Domen, *J. Am. Chem. Soc.*, 2012, **134**, 8348-8351.
3. B. Toby, *J Appl Crystallogr*, 2001, **34**, 210-213.
4. J. P. Perdew, J. A. Chevary, S. H. Vosko, K. A. Jackson, M. R. Pederson, D. J. Singh and C. Fiolhais, *Phys. Rev. B*, 1992, **46**, 6671-6687.
5. J. P. Perdew, K. Burke and M. Ernzerhof, *Phys. Rev. Lett.*, 1996, **77**, 3865-3868.
6. P. E. Blöchl, *Phys. Rev. B*, 1994, **50**, 17953-17979.
7. J. Hafner, *J. Comput. Chem.*, 2008, **29**, 2044-2078.
8. G. Kresse and J. Furthmüller, *Phys. Rev. B*, 1996, **54**, 11169-11186.
9. G. Kresse and D. Joubert, *Phys. Rev. B*, 1999, **59**, 1758-1775.
10. H. J. Monkhorst and J. D. Pack, *Phys. Rev. B*, 1976, **13**, 5188-5192.
11. J. Feng, B. Xiao, C. L. Wan, Z. X. Qu, Z. C. Huang, J. C. Chen, R. Zhou and W. Pan, *Acta Mater.*, 2011, **59**, 1742-1760.
12. M. Dey, A. Singh and A. K. Singh, *J. Phys. Chem. C*, 2021, **125**, 11548-11554.